The Effect of the Method of Canal Flare Index Calculation on Femoral Classification in Dogs: An Ex Vivo Study

Beatriz Maia Galetti, BSc[1] Caroline Ribeiro Andrade, PhD[1] Bruno Watanabe Minto, PhD[1] Luís Gustavo Gosuen Gonçalves Dias, PhD[1] Brenda Mendonça Alcântara, MSc[1] Ana Carolina Valentim Hespanha, MSc[1] Tryssia Scalon Magalhães Moi, MSc[1] Letícia Santos Goes, BSc[1]

[1] Department of Veterinary Clinic and Surgery, School of Agricultural and Veterinary Sciences, São Paulo State University, Jaboticabal, São Paulo, Brazil.

VCOT Open 2024;7:e33–e39.

Address for correspondence Beatriz Maia Galetti, BSc, Universidade Estadual Paulista, Faculdade de Ciências Agrárias e Veterinárias - Câmpus de Jaboticabal Via de Acesso Prof.Paulo Donato Castellane s/n - Jaboticabal/SP, Sao Paulo 14884-900, Brazil (e-mail: beatriz.maia@unesp.br).

Abstract

Objectives The aim of this study was to compare canal flare index (CFI) values obtained by different intracortical widths in the lesser trochanter and to evaluate their influence on femoral classification.

Methods Femur radiographic images were analysed by three evaluators that calculated the CFI using three different points in the lesser trochanter: proximal, midpoint, and distal.

Results There was no interobserver influence, but there was a difference in the CFI value and femoral classification according to the calculation method. The proximal region presents higher CFI values and only 4% of 'Stovepipe' femurs, while the distal region presents lower CFI values and 46% of 'Stovepipe' femurs.

Clinical Significance The variation in level of measurement can significantly alter femoral classification, which must be considered when the CFI is used in the surgical planning of total hip arthroplasty.

Keywords
- total hip arthroplasty
- femur
- canal flare index
- dogs
- ex vivo study

Introduction

Canine hip dysplasia (HD) is the most diagnosed orthopaedic condition in dogs and can be associated with a reduced quality of life.[1] The management of HD is remarkably challenging and ideally involves a multifactorial approach, with surgical and conservative components.[2–8] Total hip arthroplasty (THA) is a salvage procedure that can be used to treat dogs with uncontrolled clinical signs of hip arthrosis. It has been performed successfully in dogs, enabling maintenance of a functional pelvic limb with effective recovery of joint mechanisms.[3–7]

Considering the importance of the THA in the management of canine HD and a concerning rate of complications after this procedure in dogs,[9–15] in particular, femoral fractures and femoral stem subsidence,[16–20] several studies have tried to better understand the morphology of the proximal femur. These studies assist with THA surgical planning and implant selection, informing the choice of the implant in both human[8,21–24] and veterinary medicine.[16,21,22,25–28]

The canal flare index (CFI) was defined by Noble and colleagues[8] and it is widely applied in human and veterinary medicine for THA planning and femoral stem selection. The CFI is the ratio of the intracortical width at the level of the

received
May 11, 2023
accepted after revision
January 19, 2024

DOI https://doi.org/10.1055/s-0044-1782533.
ISSN 2625-2325.

Georg Thieme Verlag KG, Rüdigerstraße 14, 70469 Stuttgart, Germany

lesser trochanter to the intracortical width at the level of the isthmus and it is used as an indirect form of femoral classification.[8] In dogs, femurs can be classified into three morphological types: 'Stovepipe' (CFI $<$ 1.8), normal (1.8 $<$ CFI $<$ 2.5) and 'Champagne Fluted' (CFI $>$ 2.5) based on CFI.[16]

Use of this segmentation improves the selection of patients for THA, choice of surgical technique, and the design of the ideal femoral implant,[16,21,22,25,26,28] since accuracy of femoral stem size calculation and femoral canal matching is crucial to the initial stability of the prosthesis. Maximisation of femoral canal filling enables appropriate fixation and increases the chance for restoring normal biomechanics of the hip.[16,27,29,30] Additionally, an accurate understanding of each individual femoral characteristic enables prediction of potential complications, such as femoral stem subsidence and severe femoral fractures.[16–20] In addition to CFI, there are other factors that need to be considered when selecting patients for THA and reducing complications. It is important to understand the risk factors, such as femoral fracture, intraoperative fissures, use of uncemented stem, osteopenic bones, and others.[27,31] Bone quality can be assessed and may influence rate of potential complications and the bone mineral density can be measured through dual-energy X-ray absorptiometry.[32]

Uncemented systems are currently the most commonly used systems for THA.[3–5,15,33,34] Such systems are totally reliant on biological fixation, so implant stability in the immediate postoperative period is crucial.[17,24] Geometric fit between the femoral component and the proximal canal is essential for the success of the technique and reduction in complication rates.[15,21]

The literature describes different methods for CFI calculation with multiple anatomic regions of the femur used to measure the intracortical width.[16,26,35–38] However, due to the anatomy of the proximal metaphysis of the canine femur, there is a variation in the intracortical width at the three regions normally used to calculate the CFI (proximal, midpoint and distal aspect of the lesser trochanter), which may change the final CFI value and even the morphologic femoral classification.[24,26,35] Few studies have investigated the influence of the CFI calculation method on the final CFI value.

The aim of this study was to compare the CFI values obtained by different calculation methods involving measurement of the intracortical widths in the region of the lesser trochanter (proximal, midpoint and distal end of the lesser trochanter) and to evaluate the influence of these different measurement points (proximal, midpoint and distal end of the lesser trochanter) on the final CFI value and femoral classification.

Materials and Methods

Craniocaudal radiographic projections of the femur, obtained from 23 skeletally mature canine cadavers (mixed breeds, 40–60 kg), were used. The femurs were anatomically dissected from the specimen and positioned directly on the radiographic cassette, minimising distortion and magnification of the radiographic image. To achieve accurate positioning of the femurs, radiotransparent sponges were used for support, such that the femur rested on the condyles keeping the bone parallel to the cassette (►**Fig. 1**). Radiographs were taken with digital radiographic equipment (Siemens, São Paulo State University, Jaboticabal, Via de Acesso Prof. Paulo Donato Castellane s/n, CEP 14884-900, São Paulo, Brazil, RG150/100 gl) and a magnification indicator was positioned parallel to the femur in all projections. Right and left femurs were considered as distinct experimental units, resulting in a total sample size of 45 femurs.

The radiographic images were individually analysed by three evaluators. For each radiographic image, the evaluators measured the intracortical width at the proximal and distal ends and at the midpoint of the lesser trochanter. The intracortical width was measured at the level of the isthmus, defined as the narrowest point of the medullary canal in diaphyseal region, subjectively chosen by each evaluator (►**Fig. 2**). The ratio of intracortical widths at the different regions of the lesser trochanter and intracortical width of the isthmus determined the proximal, midpoint and distal CFI (►**Fig. 2**).

The power of the test is post-hoc and was calculated using the 'pwr.anova.test' function of the 'pwr' package. The arguments provided included the number of groups (3), the sample size in each group (135), the effect size, calculated as the ratio between the sum of squares between groups (SSB) and the total sum of squares (SST + SSB). The power of the test was calculated for a significance level of 0.05.

Descriptive analysis of the CFI variable was performed using mean and standard deviation. The data were submitted to the Shapiro-Wilk normality and Bartlet homoscedasticity tests. Contrasts within factors were obtained using Bonferroni's multiple comparisons test. All analyses was performed using R Software (R Core Team, 2020), with a significance level of 5%.

Results

The repeatability test ensured the integrity of the measurement method and the study reproducibility. In all three treatments, the power of the test was equal to or close to 0.80 (80%) (►**Table 1**) which confers reliability on the results of difference between treatments (Bonferroni) (►**Table 2**). In other words, the sample size was large enough to ensure that the results are reliable.

There was no meaningful difference between the three observers in measurements at any level ($p < 0.001$; ►**Table 3**). The agreement between the evaluators was determined using the intraclass correlation coefficient with a 95% confidence interval. However, there was a significant difference in the final CFI value between all levels, in which the mean and standard deviation were proximal 2.15 ± 0.29, midpoint 1.96 ± 0.31 and distal 1.81 ± 0.31 (►**Table 2**). In addition, it is worth noting the low standard deviation in all cases, which indicates that the mean is a good representation of the dataset (►**Table 2**).

The boxplot analysis shows that the median measurements of the observers at each region (proximal, midpoint and distal) are remarkably similar, indicating little variation in interobserver measurements. However, the median CFI values reduced from the proximal to midpoint and midpoint to distal regions, with median measurements being highest proximally and lowest distally (►**Fig. 3**).

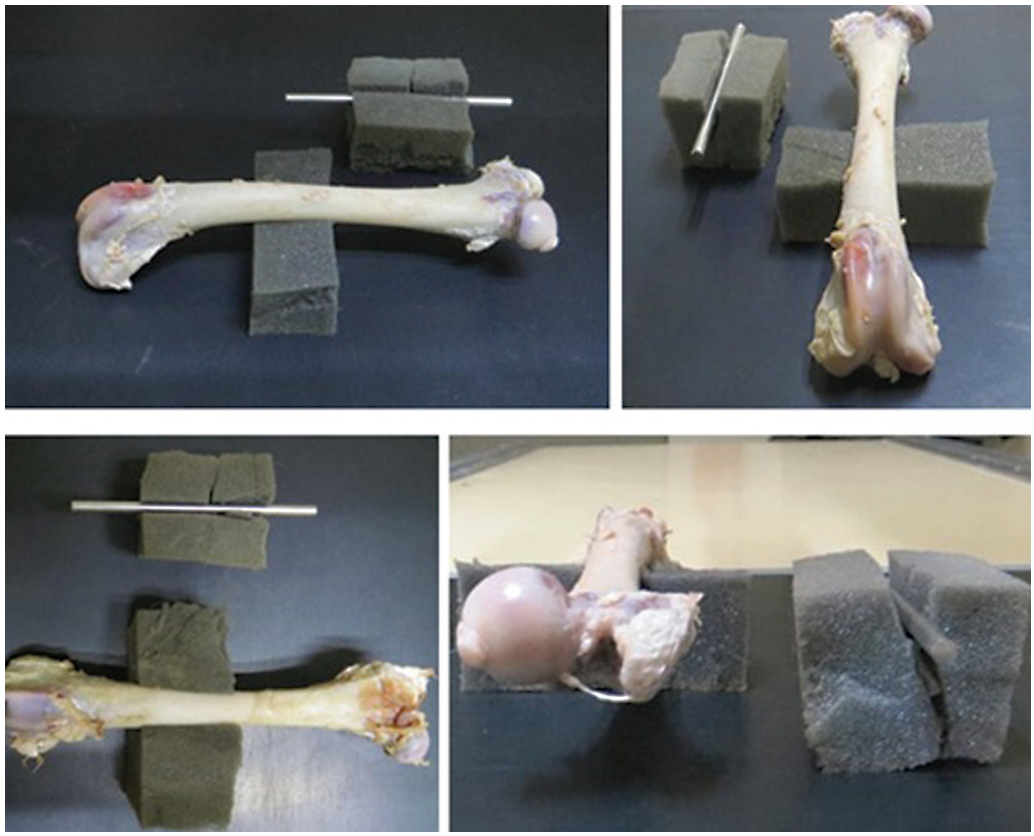

Fig. 1 Photographic images of femoral positioning to obtain the craniocaudal radiographic projection. The images also show the stainless-steel magnification marker, 10 cm long.

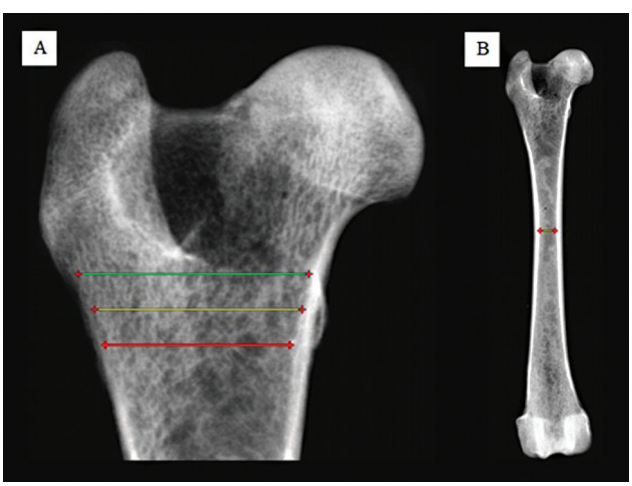

Fig. 2 Representation of the lines drawn for intracortical width at three different points in the region of the lesser trochanter: proximal end (green), midpoint (yellow) and distal end (red) (**A**). Measurement of intracortical width at the isthmus (**B**).

Table 1 Test power for analysis of the three treatments

Treatment	Sample size	Power
Proximal	135	0.83
Midpoint	135	0.83
Distal	135	0.83

►**Table 4** summarise the results for each region of the lesser trochanter used to calculate the CFI and the prevalence of each femoral classification depending on the calculation method.

As no difference was observed between the three evaluators, results were combined as follows: for the proximal level, 4% of the femurs were classified as 'Stovepipe', 22% as 'Champagne Fluted' and 74% as 'Normal' (►**Fig. 4A**); for the midpoint level, 20% of the femurs classified as 'Stovepipe', 15% as 'Champagne Fluted' and 65% as 'Normal' (►**Fig. 4B**); and for the distal level, 46% of femurs classified as 'Stovepipe', only 4% as 'Champagne Fluted' and 50% as 'Normal' (►**Fig. 4C**).

Discussion

This study demonstrated that the point chosen for endosteal measurement in the region of the lesser trochanter directly influences the final CFI value. CFI variation is associated with the different regions of measurement, but it is not associated with the different observers.

Recently, Sevil-Kilimci and Kara[38] investigated how the canine CFI is influenced by the measurement method. However, that study only investigated the influence of measurements at the proximal and midpoint regions of the lesser trochanter, while this study evaluates the influence of measurement at each of three regions of the lesser trochanter on the calculation of the CFI.

Table 2 Descriptive analysis of the canal flare index variable at the three regions for each of the observers

Treatment	Observer	*n*	Mean	SD	Min.	Máx.	Bonf.
Proximal	1	45	2.14	0.24	1.03	3.12	
	2	45	2.15	0.28	1.75	3.06	a
	3 Total	45 135	2.17 2.15	0.25 0.29	1.59 1.03	3.18 3.18	
Midpoint	1	45	1.94	0.30	0.90	2.83	
	2	45	1.96	0.31	1.60	2.70	b
	3 Total	45 135	1.98 1.96	0.28 0.31	1.45 0.90	2.77 2.83	
	1	45	1.79	0.33	1.03	2.55	
Distal	2	45	1.82	0.31	1.47	2.62	c
	3 Total	45 135	1.81 1.81	0.27 0.31	1.41 1.03	2.45 2.62	

Abbreviations: Bonf, Bonferroni's multiple comparisons test; max, maximum; min, minimum; n, number of observations; SD, standard deviation.

Table 3 Descriptive table of the intraclass correlation coefficients (ICCs) in the interobserver analyses (reproducibility)

Treatment	ICC (95% CI)	*p*-Value
Proximal	0.97 (0.94–0.99)	< 0.001
	0.97 (0.94–0.99)	< 0.001
Midpoint	0.98 (0.97–0.99)	< 0.001
	0.97 (0.93–0.98)	< 0.001
Distal	0.99 (0.98–0.99)	< 0,001
	0.97 (0.93–0.99)	< 0,001

Abbreviations: CI, confidence interval.

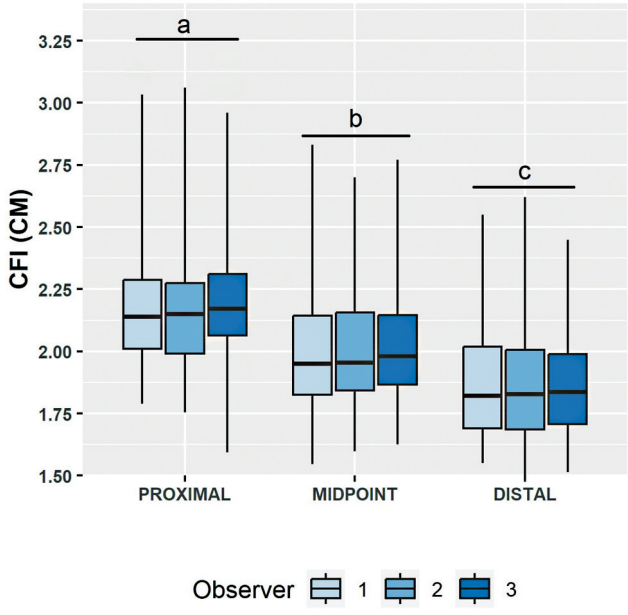

Fig. 3 Boxplot of the canal flare index (CFI) variable for the three different measurement regions and observers. The black horizontal line inside the box is the median and the black horizontal line outside the box indicates the mean plus three times the standard deviation. The ends of the box are the interquartile ranges (25 and 75% of the data). Different letters indicate statistically significant difference, according to Bonferroni's multiple comparisons test. The vertical lines indicate all the CFI values.

Table 4 Femoral classification from the calculation of the canal flare index in the proximal, midpoint and distal region of the lesser trochanter by the three observers

Treatment	Observer	Stovepipe	Normal	Champagne fluted
Proximal	1	6.7	73.3	20.0
	2	4.4	77.8	17.8
	3	4.4	75.6	20.0
Midpoint	1	22.2	66.7	11.1
	2	20.0	64.4	15.6
	3	20.0	68.9	11.1
	1	51.1	46.7	2.2
Distal	2	46.7	51.1	2.2
	3	57.8	42.2	0

In the human literature,[8] the optimal region for calculation of CFI is 20 mm above the lesser trochanter. However, in veterinary medicine there are no anatomical studies that discuss this issue. In dogs the proximal stem is placed at the metaphyseal region delimited by endosteal limits at the midpoint of the lesser trochanter. Our study observed that there was no difference between the evaluators, but that when the proximal and midpoint of lesser trochanter are used for the calculation of CFI, the populations of the three femoral types are more homogeneous (►**Fig. 4**), and the same was observed in the study by Sevil-Kilimci and Kara.[38]

In a similar study, Sevil-Kilimci and Kara[38] calculated the CFILT-I as the ratio of the endosteal width at the medial aspect of the lesser trochanter and at the isthmus resulting in 6% stovepipe, 82% normal and 12% champagne fluted. The CFIPLT-I was calculated as the ratio of the endosteal width at the proximal aspect of the lesser trochanter and at the isthmus; in this case no stovepipe femurs were observed, 55% of femurs were normal and 45% were champagne fluted. Such variation in femoral types according to the region of the

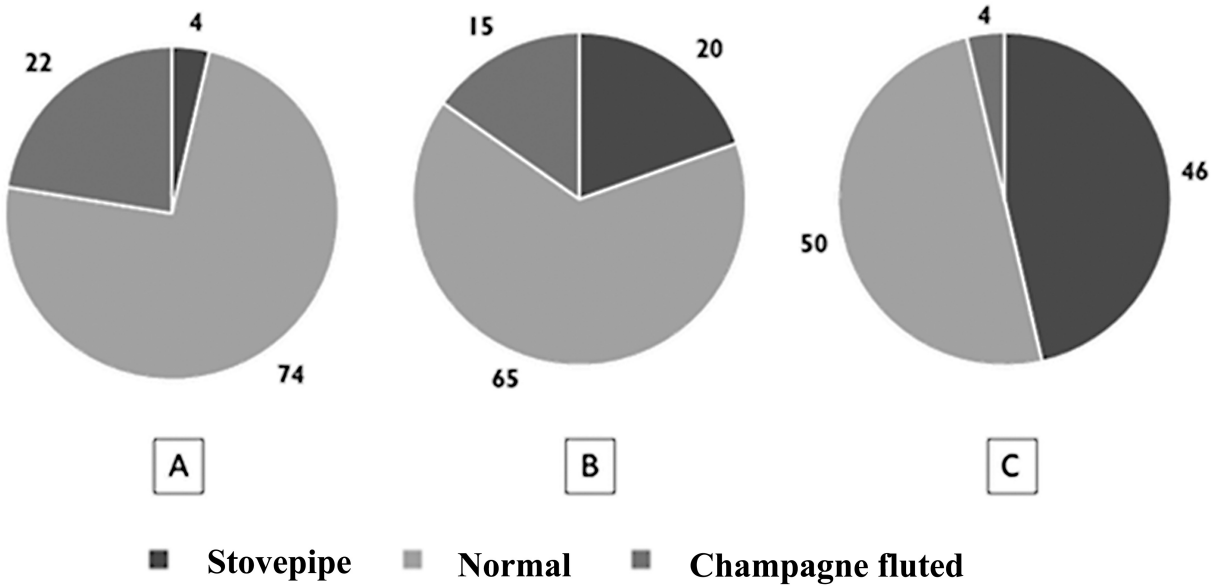

Fig. 4 Femoral classification of the three observers based on the calculation of canal flare index in the proximal (**A**), midpoint (**B**) and distal (**C**) region of the lesser trochanter.

lesser trochanter used to obtain the CFI demonstrates the influence of the calculation method on femoral classification.

In this study, the mean of proximal, midpoint and distal CFI values were 2.15, 1.96 and 1.81 respectively. In other studies, when the proximal region of the lesser trochanter is chosen to calculate the CFI, the average is 2.40[35] and 2.48.[38] The literature also reports a mean of 2.10[39] when using the midpoint region of the lesser trochanter.

Substantial differences were observed in the endosteal widths between the regions of the lesser trochanter. As the endosteal width in the proximal region of the lesser trochanter is greater than in the midpoint and in the distal region, the calculated CFI will be highest in this region and lowest in the distal region. In this study, on average, the endosteal width in the proximal region of the lesser trochanter was 9% greater than in the midpoint region and 17% greater than in the distal region. Other studies have reported an endosteal width in the proximal region of the lesser trochanter 14%[35] and 12%[38] greater than in the midpoint region and 24% greater than in the distal region.[35]

Such variation in endosteal width used for the CFI calculation results in variations in the CFI, which may change the classification of a femur. This has a direct influence on the planning of surgical procedures such as THA, because the stem is proximally sited at the diameter of the metaphyseal region, which is used to calculate the CFI.[8] It is, therefore, important to be aware, when planning THA procedures, that the CFI will vary depending on the measurement point.

To reduce potential complications after cementless THA[11,12,17,19] such as femoral fissures, fractures and subsidence of the femoral component, CFI is also important in clinical practice for the selection of the appropriate technique and implant used in THA, especially femoral systems in some situations such as a stovepipe femoral morphology. Larger patients with CFI less than 1.8, categorised as stovepipe, may require the use of cementless collared stems, a cementless stem with a lateral bolt or a cemented stem to provide protection against implant subsidence in the early postoperative and implant stabilisation periods.[40]

'Stovepipe' femurs, which have a lower CFI, are straighter than normal and 'Champagne-Fluted' femurs, which have higher CFIs, representing tapered bones with thinner structures. The use of cemented implants has been recommended in dogs with 'Stovepipe' femoral morphology, since the risks of postoperative femoral subsidence and fracture are higher.[3–5]

In this study, interobserver effects were studied by analysis of results from three observers, but there was no interobserver difference, demonstrating reliability and reproducibility of the evaluated data. Previous studies have included measurements performed by a single observer, eliminating any possibility of interobserver influence but precluding assessment of interobserver effects.[26]

The clinical positioning indicated for the calculation of the CFI is extended leg ventrodorsal radiographical positioning for standard craniocaudal femoral radiograph. de Andrade and colleagues demonstrated that the craniocaudal projection with a horizontal radiographic beam is the best approach to provide true anatomical dimensions of the canine femur, minimising the effect of the positioning artifact on the CFI values.[37] However, this study is anatomical and aimed to provide a more reliable version of the craniocaudal image of the femur.

The primary limitation of this study is that isolated femurs from cadavers were used, which allows for ideal radiographic positioning. In clinical practice, it is rarely possible to achieve optimal positioning for radiography due to pain and other positioning limitations. Thus, if performed in live animals, the measurements obtained and the final CFI values could be different from the results of this study.

The radiographic positioning of the femur used in this study is in line with the method described by Palierne and colleagues[35,36] as well as Sevil-Kilimci's study.[38] In this study, the femur was positioned directly on the radiographic cassette, supported on the condyles and kept parallel to the cassette with the aid of radiotransparent foam (►**Fig. 1**). This positioning reduced femoral angulation in relation to the radiographic cassette, removing the effects of cadaver positioning.

The study of the CFI is highly relevant since the method of measurement can potentially influence the surgeon's understanding of the geometry of the proximal femur and, consequently, affect the planning of the procedure.

Conclusion

The CFI decreased when measurements were made at the top, midpoint or bottom of the lesser trochanter.

The proximal region of the lesser trochanter is the one that relates to the proximal aspect of the stem. Calculation of CFI in this region allows us to observe a more uniform population, as used in other studies.[38]

Therefore, in THA planning, veterinary surgeons should consider the fact that canal flare measurements differ between calculation methods. Further morphological studies of the canine femur are needed to determine and standardise the CFI measurement in dogs and to better evaluate the CFI measurements influence on the complication rates.

Funding
This study was financially supported by the São Paulo Research Foundation (FAPESP).

Conflict of Interest
None declared.

Acknowledgment
The authors would like to thank São Paulo Research Foundation (FAPESP).

References

1 King MD. Etiopathogenesis of canine hip dysplasia, prevalence, and genetics. Vet Clin North Am Small Anim Pract 2017;47(04): 753–767
2 Harper TAM. Innoplant total hip replacement system. Vet Clin North Am Small Anim Pract 2017;47(04):935–944
3 DeYoung DJ, Schiller RA. Radiographic criteria for evaluation of uncemented total hip replacement in dogs. Vet Surg 1992;21(02): 88–98
4 Marcellin-Little DJ, DeYoung BA, Doyens DH, DeYoung DJ. Canine uncemented porous-coated anatomic total hip arthroplasty: results of a long-term prospective evaluation of 50 consecutive cases. Vet Surg 1999;28(01):10–20
5 Guerrero TG, Montavon PM. Zurich cementless total hip replacement: retrospective evaluation of 2nd generation implants in 60 dogs. Vet Surg 2009;38(01):70–80
6 Fitzpatrick N, Law AY, Bielecki M, Girling S. Cementless total hip replacement in 20 juveniles using BFX™ arthroplasty. Vet Surg 2014;43(06):715–725
7 Vezzoni L, Vezzoni A, Boudrieau RJ. Long-term outcome of Zürich cementless Total Hip Arthroplasty in 439 cases. Vet Surg 2015;44 (08):921–929
8 Noble PC, Alexander JW, Lindahl LJ, Yew DT, Granberry WM, Tullos HS. The anatomic basis of femoral component design. Clin Orthop Relat Res 1988;(235):148–165
9 Kwok JY, Wendelburg KL. Clinical outcomes of canine total hip replacement utilizing a BFX lateral bolt femoral stem: 195 consecutive cases (2013-2019). Vet Surg 2023;52(01):51–61
10 Dyce J, Wisner ER, Wang Q, Olmstead ML. Evaluation of risk factors for luxation after total hip replacement in dogs. Vet Surg 2000;29 (06):524–532
11 Kidd SW, Preston CA, Moore GE. Complications of porous-coated press-fit cementless total hip replacement in dogs. Vet Comp Orthop Traumatol 2016;29(05):402–408
12 Hummel DW, Lanz OI, Werre SR. Complications of cementless total hip replacement. A retrospective study of 163 cases. Vet Comp Orthop Traumatol 2010;23(06):424–432
13 Bergh MS, Gilley RS, Shofer FS, Kapatkin AS. Complications and radiographic findings following cemented total hip replacement: a retrospective evaluation of 97 dogs. Vet Comp Orthop Traumatol 2006;19(03):172–179
14 Hunter S, Dyce J, Butkus L, Olmstead ML. Acetabular cup displacement after polyethylene cement interface failure: a complication of total hip replacement in seven dogs. Vet Comp Orthop Traumatol 2003;16(02):99–104
15 Serrato SAA, Rezende CMF, Vieira GLT, Cardona LA. Coxofemoral prosthesis in canines: tissue reaction and radiographic evaluation methods. J of Vet Med 2008;15:9–19
16 Rashmir-Raven AM, DeYoung DJ, Abrams CF Jr, Aberman HA, Richardson DC. Subsidence of an uncemented canine femoral stem. Vet Surg 1992;21(05):327–331
17 Pernell RT, Gross RS, Milton JL, et al. Femoral strain distribution and subsidence after physiological loading of a cementless canine femoral prosthesis: the effects of implant orientation, canal fill, and implant fit. Vet Surg 1994;23(06):503–518
18 Liska WD. Femur fractures associated with canine total hip replacement. Vet Surg 2004;33(02):164–172
19 Ganz SM, Jackson J, VanEnkevort B. Risk factors for femoral fracture after canine press-fit cementless total hip arthroplasty. Vet Surg 2010;39(06):688–695
20 Mitchell MM, Hudson CC, Beale BS. Comparison of femoral stem subsidence between three types of press-fit cementless total hip replacement in dogs. Vet Surg 2020;49(04):787–793
21 Tawada K, Iguchi H, Tanaka N, et al. Is the canal flare index a reliable means of estimation of canal shape? Measurement of proximal femoral geometry by use of 3D models of the femur. J Orthop Sci 2015;20(03):498–506
22 Casper DS, Kim GK, Parvizi J, Freeman TA. Morphology of the proximal femur differs widely with age and sex: relevance to design and selection of femoral prostheses. J Orthop Res 2012;30 (07):1162–1166
23 Husmann O, Rubin PJ, Leyvraz PF, de Roguin B, Argenson JN. Three-dimensional morphology of the proximal femur. J Arthroplasty 1997;12(04):444–450
24 Rubin PJ, Leyvraz PF, Aubaniac JM, Argenson JN, Estève P, de Roguin B. The morphology of the proximal femur. A three-dimensional radiographic analysis. J Bone Joint Surg Br 1992;74 (01):28–32
25 Meltzer LM, Dyce J, Leasure CS, Canapp SO Jr. Case factors for selection of femoral component type in canine hip arthroplasty using a modular system. Vet Surg 2022;51(02):286–295
26 Sevil-Kilimci F, Kara ME. The geometry of the proximal femoral medullary canal in german shepherd and kangal dogs. J Faculty Veterinary Med Istanbul Univers 2017;43(01):52–60

27 Pugliese LC. Proximal femoral morphology and bone quality assessment in dogs. [Thesis (Master of Science)]. Columbus: Graduate School of The Ohio State University; The Ohio State University; 2014
28 Sumner DR Jr, Devlin TC, Winkelman D, Turner TM. The geometry of the adult canine proximal femur. J Orthop Res 1990;8(05):671–677
29 Worden NJ, Ash KJ, Ordway NR, et al. Radiographic and biomechanical assessment of three implant designs for canine cementless total hip replacement. Vet Comp Orthop Traumatol 2020;33(06):417–427
30 Worden NJ, Ash KJ, Ordway NR, et al. Effect of stem positioning on biomechanical performance of a novel cementless short-stem canine total hip implant. Vet and Comp Orthop and Traumatol. 2022;35(00):(01):001–009
31 Haidukewych GJ, Stewart C. "Intraoperative Fractures During Total Hip Arthroplasty: See It Before It Sees You.". Seminars in Arthroplasty. Vol. 22. No. 2. WB Saunders, 2011
32 Yeung Y, Chiu KY, Yau WP, Tang WM, Cheung WY, Ng TP. Assessment of the proximal femoral morphology using plain radiograph-can it predict the bone quality? J Arthroplasty 2006;21(04):508–513
33 Chen PQ, Turner TM, Ronnigen H, Galante J, Urban R, Rostoker W. A canine cementless total hip prosthesis model. Clin Orthop Relat Res 1983;(176):24–33
34 Hanson SP, Peck JN, Berry CR, Graham J, Stevens G. Radiographic evaluation of the Zurich cementless total hip acetabular component. Vet Surg 2006;35(06):550–558
35 Palierne S, Asimus E, Mathon D, Meynaud-Collard P, Autefage A. Geometric analysis of the proximal femur in a diverse sample of dogs. Res Vet Sci 2006;80(03):243–252
36 Palierne S, Mathon D, Asimus E, Concordet D, Meynaud-Collard P, Autefage A. Segmentation of the canine population in different femoral morphological groups. Res Vet Sci 2008;85 (03):407–417
37 de Andrade CR, Minto BW, Dreibi RM, et al. Accuracy in determining canal flare index using different radiographical positions for imaging canine femurs. Vet Comp Orthop Traumatol 2019;32 (03):234–240
38 Sevil-Kilimci F, Kara ME. Canal flare index in the canine femur is influenced by the measurement method. Vet Comp Orthop Traumatol 2020;33(03):198–204
39 Christopher SA, Kim SE, Roe S, Pozzi A. Biomechanical evaluation of adjunctive cerclage wire fixation for the prevention of periprosthetic femur fractures using cementless press-fit total hip replacement. Vet J 2016;214:7–9
40 Schiller TD. Biomedtrix total hip replacement systems: an overview. Vet Clin North Am Small Anim Pract 2017;47(04):899–916